Gravity center change of carbon emissions in Chinese residential building sector
Differences between urban and rural area

Wang, Jiebing; You, Kairui; Qi, Lingling; Ren, Hong

DOI
10.1016/j.egyr.2022.08.208

Publication date
2022

Document Version
Final published version

Published in
Energy Reports

Energy Reports 8 (2022) 10644–10656

Contents lists available at ScienceDirect

Energy Reports

journal homepage: www.elsevier.com/locate/egyr

Research paper

Gravity center change of carbon emissions in Chinese residential building sector: Differences between urban and rural area

Jiebing Wang [a,1], Kairui You [b,1,*], Lingling Qi [a], Hong Ren [a]

[a] School of Management Science and Real Estate, Chongqing University, Chongqing, 400044, PR China
[b] Faculty of Architecture and The Built Environment, Delft University of Technology, Delft 2628BL, The Netherlands

ARTICLE INFO

Article history:
Received 30 May 2022
Received in revised form 25 July 2022
Accepted 15 August 2022
Available online xxxx

Keywords:
Residential building
Carbon emissions
Gravity center model
Spatial–temporal logarithmic mean Divisia index
Tapio decoupling analysis

ABSTRACT

In China, dynamic spatial–temporal evolution and urban–rural gap in carbon emissions of residential building sector are crucial for understanding the current state, which is faced with great challenges related to emission mitigation. To overcome the challenge, this study employed the gravity center model to explore spatial–temporal evolution of carbon emissions and analyzed the driving factories leading the differences between urban residential buildings and rural residential buildings via decomposition analysis. Meanwhile, Tapio decoupling index is used to predict the future movement of the gravity center. Our results indicated that: (i) the carbon emissions gravity center of both residential building types tends to move south; (ii) the northeast and northwest regions play the largest role in driving the gravity center movement of urban residential buildings and rural residential buildings, respectively; (iii) per capita disposable income is the primary factors affecting the gravity center movement. (iv) the gravity center of both residential building types might tend to move westward in the future. Overall, this study attempts to remedy the current lack of research pertaining to spatial–temporal evolution laws governing carbon emissions in the Chinese residential building sector and provides a reference point for the implementation of targeted urban and rural emission reduction policies.

1. Introduction

In 2018, China's building sector-related carbon emissions reached 2.1 billion tons, accounting for 21.9% of the national carbon emissions, of which residential building-related carbon emissions accounted for 63% of the total building carbon emissions (CABEE, 2020). At present, building-related energy consumption per capita in China is far lower than that in developed countries (THUBERC, 2020), indicating that energy consumption and carbon emissions of Chinese residential buildings will continue to show sustained growth as population increases (Delmastro et al., 2015)and residential income level rises (Huo et al., 2021b) in the future. However, many studies have contended that the residential building sector, which shows great emission reduction potential (Ma et al., 2020; Zhou et al., 2018), may reap economic benefits via the existing emission reduction technologies (Schäuble et al., 2020; Yan et al., 2019). Tan et al. (2018) have presented a best emission mitigation scenario in which the Chinese residential building sector reaches a turning point and achieves peak emission before 2030, while McNeil et al. (2016) have argued that effective building codes may help reduce residential building-related carbon emissions in China by half. In this scenario, actions taken by the Chinese residential building sector towards emission reduction may play a significant role in enabling China to fulfill its climate goals of carbon peak and neutrality.

At present, the total emissions and intensity associated with the residential building sector in China have shown a significant spatial difference under the influence of various factors. Cong et al. (2015) concluded that the carbon emissions increase more in regions with lower temperatures under the influence of the same factors, Huo et al. (2021a) assumed that the development of urbanization showed a higher promoting effect on the carbon emissions of urban residential building in the central region than in the other two region groups, and Li et al. (2021a) proposed that energy efficiency policy plays a crucial role in the disparities of per-capita CO2 emissions. Some researchers have proposed that differences in development may affect the time and intensity of the emission peak in each region (Chen and Chen, 2019; Liang et al., 2019). Differences across the urban–rural gradient in relation to the built environment also exert an effect on policy making (Halleck Vega et al., 2022). Therefore, an analysis of the spatial–temporal evolution of building sector-related emissions, which provides background information useful for achieving specific regional carbon emission-reduction targets, is needed (Wang

* Corresponding author.
E-mail addresses: 202003021006@cqu.edu.cn (J. Wang), K.You@tudelft.nl (K. You), Lynn.l.qi@cqu.edu.cn (L. Qi), renhong@cqu.edu.cn (H. Ren).
[1] These authors contributed equally to this work.

https://doi.org/10.1016/j.egyr.2022.08.208

Nomenclature

Abbreviations

CEGC	Carbon emissions gravity center
CI	Carbon intensity per floor space
CV	Coefficient of variation
kgce	Kilogram of standard coal equivalent
$MtCO_2$	Mega-tons of carbon-dioxide
RRB	Rural residential buildings
ST-LMDI	Spatial–temporal logarithmic mean Divisia index
URB	Urban residential buildings

Symbols

C	Carbon emissions of residential building operation
CR	Contribution rate to the change of carbon emissions
E	Energy consumption of residential building operation
EE	Economic efficiency of residential buildings to resident income
EF	Carbon emissions factors
EI	Energy intensity per unit floor space
ES	Energy structure
F	Floor spaces of residential building
L	Moving distance of the gravity center
MS	Marginal contribution to the movement of the gravity center
P	Population
PY	Per capita disposable income
S	Contribution to the movement of the gravity center
SR	Contribution rate to the movement of the gravity center
TY	Disposable income of residents
X	Longitude of carbon emissions gravity center
x	Longitude of capital city
Y	Latitude of carbon emissions gravity center
y	Latitude of capital city
ρ	Conversion coefficient between the geographic coordinate system and spatial projection coordinate system.
φ	Decouple elasticity coefficient

et al., 2020a). Based on the current situation, we addressed the following four issues:

- What are the laws governing the spatial–temporal evolution of residential building carbon emissions in China?
- What differences exiting between the spatial–temporal emissions laws that apply to urban and rural residential buildings?
- What factors driving these differences?
- How to formulate specific policies according to evolutionary trends anticipated in spatial–temporal emissions?

Previous studies have used various methods to investigate the characteristics pertaining to the spatial–temporal distribution of building sector-related carbon emissions, with econometric analysis and index measurement being the most common methods. Econometric analysis is mainly used to explore the impact of factors that drive building-related carbon emissions in different regions. For example, through the STIRPAT model, a flexible and universal method used to investigate the human impact on the environment that allows new influencing factors can be added to the model framework according to the characteristics of each study (Wu et al., 2021a), Huo et al. (2020) analyzed the correlation between carbon emissions associated with residential buildings in urban area and development of urbanization in the central, western, and eastern regions of China. In addition, the spatial econometric model could test whether carbon emissions exit spatial dependence and autocorrelation pattern under the influence of external environment. In detailed, Shi et al. (2020) concluded that the carbon emissions intensity of URB in China had a spatial autocorrelation from 2000 to 2016 with different degrees impact of economics and geographic location. Wen et al. (2020) extended that there were significant spatial dependence and clustering characteristics in provincial construction carbon emissions when considering the technological innovation factors.

On the other hand, because econometric analysis is generally more suitable for analyzing relationships among factors rather than quantifying the degree of spatial differences and the causes of such disparities, many studies have opted to calculate the inequality index to evaluate the spatial distribution of carbon emissions. Commonly used relevant indexes include the Gini index (Zhang and Wang, 2017), Zenga index (Wang et al., 2020a) and Theil index (Fan et al., 2020). The above index models can describe the differences of research objects without complex construction process, but they can only express the degree of differences through the numerical values, rather than intuitively show the information in geographical space. Among these, the Theil index has been used to study the more significant differences in building sector-related emissions by decomposing the differences and dividing regional differences into differences within the region and the difference between regions (Wang et al., 2021), either alone or in combination with the decomposition method from the perspective of emission efficiency (Liu and Wang, 2019) and building types (Li et al., 2021a).

The gravity center model is an effective analytical method that is used to explore temporal–spatial distribution characteristics. This method accurately and concisely describes the distribution law of elements with a reasonable combination of time and space (Balsa-Barreiro et al., 2019). With increasing attention being directed at uneven development, this model was quickly introduced into the field of social economics and is widely applied to the research related to economy (Fu et al., 2011), energy (Zhang et al., 2012), land use (Li et al., 2020b) and environment (Ma et al., 2019; Wang et al., 2020b). To the best of our knowledge, only a few studies have applied this method to the spatiotemporal evolution analysis of building sector-related carbon emissions.

In an attempt to resolve the above-mentioned four issues, this study used the gravity center concept to analyze the laws governing spatial–temporal changes in residential building sector-related carbon emissions in China. Next, we used the Shapley and ST-LMDI decomposition model to further analyze the main factors driving the movement of gravity centers and determine possible reasons for the differences observed between urban–rural building sectors. Finally, the decoupling model was used to predict the future evolution trend of carbon emissions gravity center (CEGC) of urban residential buildings (URB) and rural residential buildings (RRB). The contributions made by this study are as follows: (1) Identification of the migration of the gravity center of carbon emissions in the residential building sector; (2) analysis of factors driving gravity center migration tracks and assessment

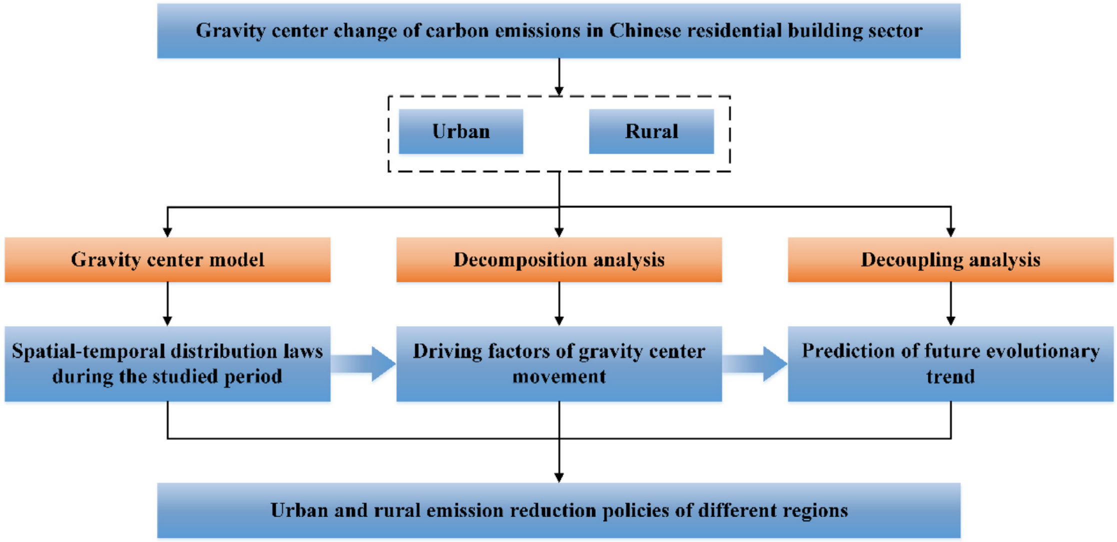

Fig. 1. Research framework of gravity center change analysis.

of future trends; (3) analysis of the differences between carbon emissions in urban and rural area in China.

The subsequent parts of the study are arranged as follows: Section 2 presents the materials and methods, including the derivation of the main models, definition of the variables, and data resources. Section 3 discusses the first three issues: Section 3.1 maps the spatial–temporal distribution of residential building emissions in China, Section 3.2 shows the different gravity center tracks of urban and rural residential buildings emissions, Section 3.3 analyzes the factors driving gravity center movement with the Shapley value and decomposition results. Section 4 tests the Tapio decoupling status between carbon emissions and key driving factors, then gives a reasonable prediction of future trend to answer the last issue, Section 5 delivers result-based conclusions and policy recommendations for regional development. Fig. 1 shows the schematic overview of the research framework.

2. Materials and methods

2.1. The gravity center model

This paper introduces the concept of using the gravity center model to analyze the carbon emissions spatial–temporal law governing the URB and RRB over time in China (issues 1 and 2 as stated in the introduction). The gravity center concept, which is based on the fulcrum that maintains balance, arises from the mechanical field of physics. The movement of the gravity center indicates that the densities of some parts have changed, allowing the gravity center model to accurately evaluate the characteristics of spatial change associated with the development of regional factors (Grether and Mathys, 2010; Harris et al., 2011). In recent years, various studies exploring carbon emission reduction have applied this model to analyze carbon emissions in various industries (Li et al., 2020a; Meng et al., 2021). The general method for calculating the gravity center is shown in Eq. (1).

$$X = \sum_{i=1}^{I} C_i x_i / \sum_{i=1}^{I} C_i,\ Y = \sum_{i=1}^{I} C_i y_i / \sum_{i=1}^{I} C_i \tag{1}$$

where X and Y, respectively, denote the longitude and latitude of gravity center. i represents different research units, and I is the total number of research units, which specifically indicates 30 provincial administrative regions in China (except Hong Kong, Macao, Taiwan, and Tibet) for this study. C_i represents total carbon emissions released from the URB and RRB. x_i and y_i are the longitude and latitude of the gravity center of each province, respectively, and the geometric center coordinates or representative location coordinates are generally selected, which incorporate the coordinates of each provincial capital city for calculation in this study.

The moving distance of the gravity center is an important measurement index used to analyze the gravity center migration trajectory, and the formula for its calculation is as follows:

$$L_{T-t} = \rho \times [(X^T - X^t)^2 + (Y^T - Y^t)^2]^{\frac{1}{2}} \tag{2}$$

where(X^T, Y^T)and(X^t, Y^t) represent gravity center coordinates of carbon emissions in different years, L_{T-t} denotes the moving distance of the gravity center from year T to year t, and constant ρ = 111.111 km indicates conversion between the geographic coordinate system and spatial projection coordinate system.

2.2. Shapley decomposition model

This model was used to determine the factors driving CEGC movement (issue 3 mentioned in the introduction). The Shapley value, which comes from cooperative game theory, is used to solve the distribution issues affecting the cooperative benefits or costs of participants (Shapley, 1953). Based on the Shapley value, Shorrocks (1999) constructed a general decomposition process, termed the Shapley decomposition. This allows all influencing factors to be included in the determinants of dependent variables in a nonlinear form and satisfies symmetry and accuracy (Yu et al., 2014). Using the Shapley decomposition, Han et al. (2015) analyzed how the household characteristics affect the household embedded carbon emissions, and Wu et al. (2021b) explored the impact of trade intensity on the per capita carbon emissions under the belt and road initiative. Additionally, several researchers assigned the carbon emissions quotas to the China's different regions according to the Shapley value (Li et al., 2021b; Zhang et al., 2014). As the decomposition of the gravity center is essentially nonlinear, this study uses the decomposition method based on the Shapley value to determine the contribution of different regions to the movement of the CEGC of the residential building sector.

This method uses the marginal contribution of each region to the gravity center movement to measure its impact on the center of gravity migration. Specifically, assuming that the studied area

N is composed of n small regions, that is, $N = \{1, 2, \ldots, j, \ldots, n\}$, the marginal contribution of region j to the movement of the gravity center can be expressed as follows:

$$MS_X^j = \Delta X(N) - \Delta X\,(N/\{j\})\,, MS_Y^j = \Delta Y(N) - \Delta Y\,(N/\{j\}) \quad (3)$$

where ΔX and ΔY represents the relative movement of the gravity center in longitude and latitude direction respectively. At this time, the result does not meet the accuracy of regional contribution; that is, the total marginal contribution of each region is not necessarily equal to the total movement, and the arrangement order of n regions need to be considered. When region j is on the order of m, the arrangement order of all regions $\sigma = (\sigma_1, \sigma_2, \ldots, \sigma_{m-1}, \sigma_m = j, \ldots, \sigma_n)$, define $(m-1)$ regions set in front of j as $Pre^j(\sigma) = (\sigma_1, \sigma_2, \ldots, \sigma_{m-1})$, then under this arrangement, the marginal contribution of region j is as follows:

$$MS_X^j(\sigma) = \Delta X\left(Pre^j(\sigma) \cup \{j\}\right) - \Delta X\left(Pre^j(\sigma)\right) \quad (4)$$

$$MS_Y^j(\sigma) = \Delta Y\left(Pre^j(\sigma) \cup \{j\}\right) - \Delta Y\left(Pre^j(\sigma)\right) \quad (5)$$

In Eqs. (4) and (5), the sum of the contributions of all regions under this arrangement is the total movement, which meets the accuracy requirements. However, when the arrangement order changes, the contribution of region j also changes, which does not meet the symmetry. This issue is solved by considering the average contribution value of region j for all permutation cases, $\prod n$. Then, the Shapley value of region j to the movement of the gravity center is as follows:

$$\begin{aligned} S_X^j &= \frac{1}{n!}\sum_{\prod n} MS_X^j(\sigma) \\ &= \frac{1}{n!}\sum_{\prod n} \Delta X\left(Pre^j(\sigma) \cup \{j\}\right) - \Delta X\left(Pre^j(\sigma)\right) \end{aligned} \quad (6)$$

$$\begin{aligned} S_Y^j &= \frac{1}{n!}\sum_{\prod n} MS_Y^j(\sigma) \\ &= \frac{1}{n!}\sum_{\prod n} \Delta Y\left(Pre^j(\sigma) \cup \{j\}\right) - \Delta Y\left(Pre^j(\sigma)\right) \end{aligned} \quad (7)$$

The contributions defined by Eqs. (6) and (7) satisfy both accuracy and symmetry, where S_X^j, S_Y^j represents the contribution of region j to the gravity movement of CO_2 emissions in the longitude and latitude directions, respectively. Furthermore, the index of contribution rate can reflect the degree of the movement of the gravity center caused by the region j, which can be defined as follows:

$$SR_X^j = S_X^j/\Delta X, SR_Y^j = S_Y^j/\Delta Y \quad (8)$$

2.3. The spatial–temporal LMDI model

In this section, the spatial–temporal logarithmic mean Divisia index (ST-LMDI) decomposition method was used to further discuss the factors affecting the change in residential building carbon emissions in each region to address the issue (3). LMDI is an important method to analyze the driving factor of carbon emissions (Ang et al., 2016), with features such as no residuals or residual values, total decomposition, and multiplication decomposition with addition (Jiang et al., 2020). ST-LMDI is the latest development of LMDI, which can better overcome the shortcomings of inaccuracy and low efficiency of traditional decomposition methods in a space–time comparison (Shi et al., 2019). The ST-LMDI method is more convenient and accurate for comparisons across time and region.

According to the classical Kaya identity, carbon emissions are mainly affected by factors such as technology, affluence, and population (Kaya, 1989). According to recent research, more extended forms of Kaya have been proposed to evaluate the roles of driving factors for emissions (Li et al., 2022). For this study, the residential building carbon emissions of region j, C_j, can be expressed as the following extended Kaya identity model:

$$\begin{aligned} C_j &= \sum_{k=1}^{K} C_{jk}/E_{jk} \times E_{jk}/E_j \times E_j/F_j \times F_j/TY_j \times TY_j/P_j \times P_j \\ &= \sum_{k=1}^{K} EF_{jk} \times ES_{jk} \times EI_j \times EE_j \times PY_j \times P_j \end{aligned} \quad (9)$$

where k represents the type of energy consumed by residential buildings in the operation stage, the direct primary energy of various fossil energy sources (coal, oil and natural gas), and secondary energy (electricity and heating) are considered. In detailed, heating generation technologies include gas-fired, coal-fired and cogeneration boiler, and electricity generation technologies include fired boiler and renewable energy (You et al., 2021). $EF_{jk} = C_{jk}/E_{jk}$, $ES_{jk} = E_{jk}/E_j$ indicate the carbon emissions factors and energy structure of the k_{th} energy in region j, respectively; $EI_j = E_j/F_j$ denotes the energy intensity per unit floor space of residential buildings in region j; $EE_j = F_j/TY_j$ represents the economic efficiency of residential buildings to the resident income in region j; $PY = TY_j/P_j$ refers to the per capita income of region j; and P_j is the population of region j. All the above indicators take the corresponding data of urban and rural areas according to the type of residential building.

In ST-LMDI decomposition, a reference region is constructed using the arithmetic mean of all variable values of all provinces and years in the sample, which is recorded as region u, and its carbon emissions level is C_u.

When $t = 0$ and $t = T$, the difference in residential building carbon emissions between region j and referent region u can be decomposed into the difference of the above-mentioned six main factors between region j and reference region u, as follows:

$$\begin{aligned} \Delta C_{j0-u} &= \Delta C_{j0} - \Delta C_u \\ &= \Delta EF_{j0-u} + \Delta ES_{j0-u} + \Delta EI_{j0-u} \\ &\quad + \Delta EE_{j0-u} + \Delta PY_{j0-u} + \Delta P_{j0-u} \end{aligned} \quad (10)$$

$$\begin{aligned} \Delta C_{jT-u} &= \Delta C_{jT} - \Delta C_u \\ &= \Delta EF_{jT-u} + \Delta ES_{jT-u} + \Delta EI_{jT-u} \\ &\quad + \Delta EE_{jT-u} + \Delta PY_{jT-u} + \Delta P_{jT-u} \end{aligned} \quad (11)$$

From $t = 0$ to$t = T$, the change of carbon emissions of regional j can be decomposed into:

$$\begin{aligned} \Delta C_{jT-j0} &= \Delta C_{jT} - \Delta C_u - \left(\Delta C_{j0} - \Delta C_u\right) \\ &= \Delta C_{jT-u} - \Delta C_{j0-u} \\ &= \Delta EF_{jT-j0} + \Delta ES_{jT-j0} + \Delta EI_{jT-j0} \\ &\quad + \Delta EE_{jT-j0} + \Delta PY_{jT-j0} + \Delta P_{jT-j0} \end{aligned} \quad (12)$$

Thus, during the period from $t = 0$ to $t = T$, every parameter (e.g., ΔEF) on the right side of Eq. (12) can be further expressed as:

$$\Delta EF_{jT-j0} = \sum_{k=1}^{K}[L\left(C_{jk,T}, C_{k,u}\right) ln\frac{EF_{jk,T}}{EF_{k,u}} - L\left(C_{jk,0}, C_{k,u}\right) ln\frac{EF_{jk,0}}{EF_{k,u}}] \quad (13)$$

where:

$$L\left(C_{jk,T}, C_{k,u}\right) = \frac{C_{jk,T} - C_{k,u}}{lnC_{jk,T} - lnC_{k,u}} \quad (14)$$

Fig. 2. The eight comprehensive economic zones in China.

$$L\left(C_{jk,0}, C_{k,u}\right) = \frac{C_{jk,T} - C_{k,u}}{lnC_{jk,T} - lnC_{k,u}} \tag{15}$$

Similarly, the contribution rate of every factor (e.g., ΔEF) to the change of carbon emissions during the period from $t = 0$ to $t = T$ can be expressed as follows:

$$CR^{j}_{EF} = \Delta EF_{jT-j0}/\Delta C_{jT-j0} \tag{16}$$

2.4. Data source and processing

The data in this paper cover 30 provinces in China (except Hong Kong, Macao, Taiwan, and Tibet) from 2005 to 2018, wherein the entire country is divided into eight comprehensive economic zones (Zhang et al., 2021). The scope of each region is shown in Fig. 2.

Based on the method proposed by the China building energy consumption calculation method (CBECM) (Huo et al., 2018), the amount of each type of energy consumed in the building sector, including primary energy (coal, oil, natural gas) and secondary energy (electricity, heating), is obtained by splitting the China's energy balance sheet. The emission factors for electricity and heating are also calculated through the splitting of the energy balance sheet (You et al., 2021). The final carbon emission is the sum of the product of various energy consumption and corresponding emission factors. The floor space data, which was obtained from the study of Huo et al. (2019), is estimated by using building stock turnover model. Coordinates of the provincial capital city were extracted using a Baidu map. Relevant income and population data were obtained from the *China Statistical Yearbook* (NBS, 2019). The income data, specifically, are based on the year 2005 as constant prices, and the resident population at the end of the year in urban and rural areas of each region is considered as population data.

3. Results

3.1. Analysis of the distribution of residential building-related carbon emissions in China

Changes in the trends of carbon emissions and the corresponding intensity per floor space (CI) of URB and RRB from 2005 to 2018 are shown in Fig. 3. The results show that carbon emissions of URB come from the consumption of primary energy, electricity generation, and central heating, whereas the carbon emissions of RRB do not include central heating. Both emissions of two types residential buildings maintained continuous growth during the study period mainly due to the increase in electricity consumption. Furthermore, the primary energy consumption of URB decreased significantly from 2013, but that of RRB did not present significant change and was always higher than URB, implying that the energy consumption structure and technology of RRB still need further improvement.

Compared with the total emissions, the CI showed a change in trends. More specifically, the CI of URB, which reached a maximum of 23.03 kgce/m^2 in 2012, began to gradually decline and reached 15.74 kgce/m^2 in 2018 (lower than the 21.10 kgce/m^2 seen in 2005), showing an obvious "Inverted U" distribution. However, the CI of RRB increased from 12.62 kgce/m^2 in 2005 to 18.35 kgce/m^2 in 2017. Although the growth rate slowed down after 2012 and showed a downward trend in 2018, it was still higher than the intensity value in most years. These results indicated, to some extent, that the initiation of energy-saving transformations in new buildings and existing buildings, which was vigorously promoted during the 12th Five Year Plan period, has vastly improved the energy efficiency of URB (Huo et al., 2020), while the CI in rural areas continues to increase.

Differences between the average levels and spatial distribution patterns of residential building-related carbon emissions in China from 2005 to 2018 are shown in Fig. 4. The yearly average carbon

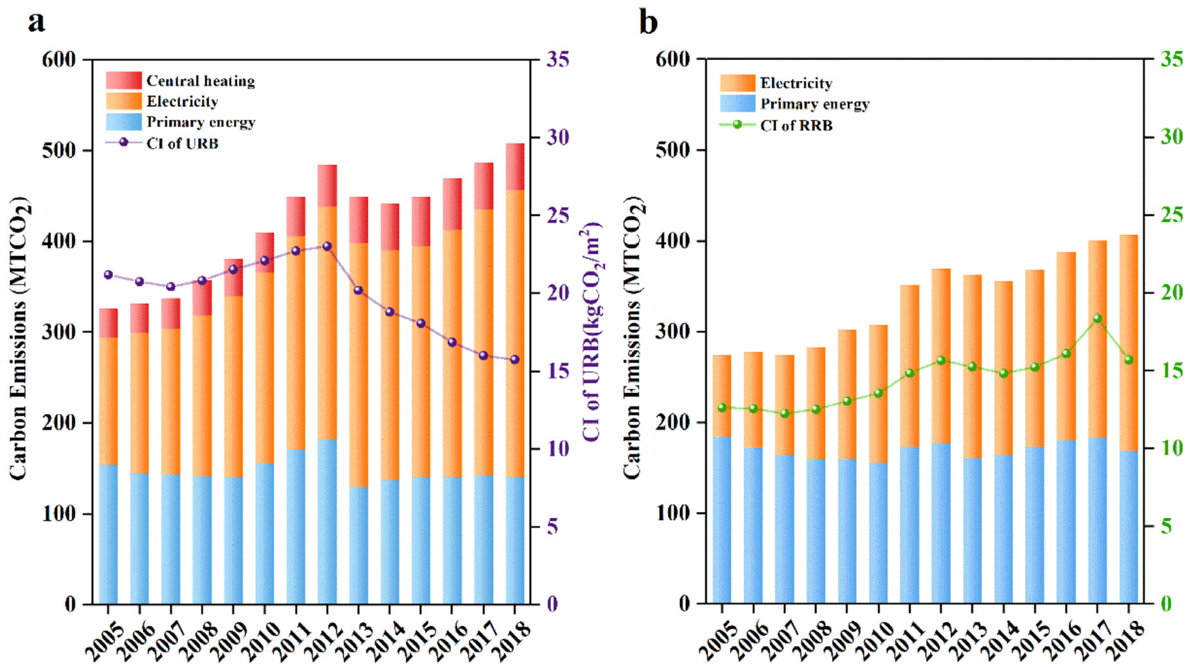

Fig. 3. Historical tendency of carbon emissions and intensity per floor space (CI) of URB (a) and RRB (b) in 2005–2018.

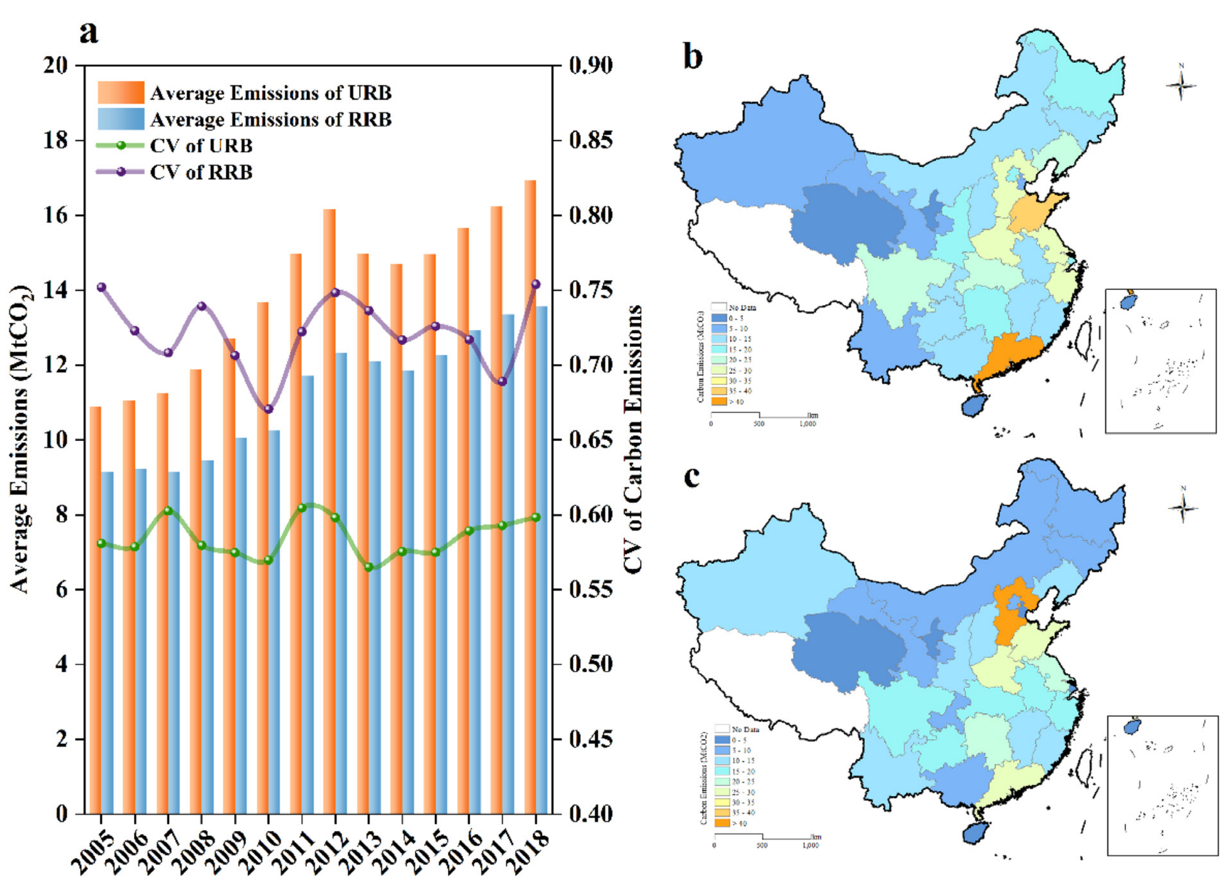

Fig. 4. Spatial distribution characteristics of carbon emissions from URB and RRB. (a) represents the mean value and coefficient of variation (CV) of carbon emissions from URB and RRB during 2005–2018. (b - c) represent the carbon emissions spatial distribution of URB and RRB, respectively, in 2018.

emissions of URB were higher than those of RRB, while the coefficient of variation (CV) of the URBs was lower than that of RRBs, indicating that the unbalanced regional development characteristics of RRB-related carbon emissions were more obvious (Fig. 4a). The respective 2018 carbon emissions from the URB and RRB in each province are shown in Figs. 4b and 3c. Firstly, with regards to the spatial distribution of the URB, the province with the highest emissions was Guangdong Province (46.21 Mt CO_2)

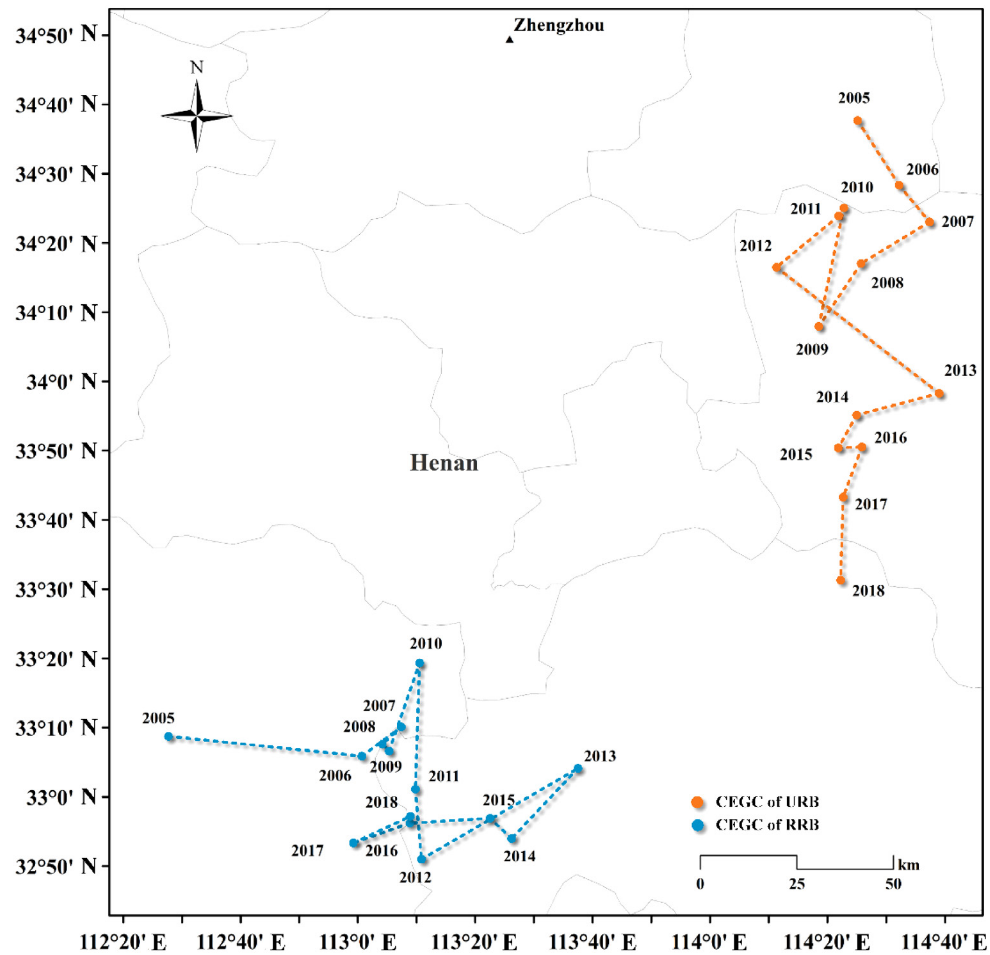

Fig. 5. CEGC migration tracks of residential building sector in China from 2005–2018.

while that with the lowest emissions was Qinghai (3.31 Mt CO_2), with emission levels in the eastern region being higher than those in the western region. Secondly, for RRB, the province with the highest emissions was Hebei Province (47.80 Mt CO_2), while that with the lowest emissions was Hainan (1.62 Mt CO_2), with the provinces with higher levels of emissions being concentrated in the eastern region.

3.2. Gravity center movement

The movement of the CEGC of URB and RRB in China from 2005 to 2018 is shown in Fig. 5. The gravity center represents the equilibrium between the weight of each particle (Sun et al., 2022), according to direction and distance of the gravity center movement, the temporal and spatial characteristics of carbon emission changes in different regions can be investigated easily. Notably, the gravity center tracks of both were located in Henan and deviated from the geometric center of China (located in Gansu Province), implying that the carbon emissions from residential buildings in the eastern region were higher than those in the western region.

The CEGC of the URB and RRB show significant differences in both location and the direction of migration. Firstly, in terms of the distribution range of coordinates, the coordinates of CEGC of the URB each year are located to the northeast of the RRB, which is related to the high level of urbanization in the eastern and northeastern regions. Secondly, in regard to the direction of gravity center migration, the emission gravity center of the URB changed markedly in the latitude direction and basically maintained a trend of rapid southward movement from 2005 to 2018, with a total of 1.1° offset, while in the longitude direction, it fluctuated slightly and moved 0.18° to the west, with the overall distance gravity center moving 286.63 km. By contrast, the emission gravity center change in RRB was mainly reflected in the longitude direction, which moved eastward by 0.67° and southward by 0.23° from 2005 to 2018, and the overall distance migrated was 322.91 km, indicating that the average moving speed of the CEGC of RRB was faster than that of URB.

Consistency in the migration of the two gravity center tracks to the south proves that China's development gravity center moves south as a whole, which is in agreement with the conclusions reached by current research studies exploring the socio-economic gravity center (Liang et al., 2021). The sharp conversion in the CEGC of RRB in the longitudinal direction indicated the presence of an obvious spatial imbalance and time asynchrony in development between rural areas in the eastern and western regions of China.

3.3. Analysis of the factors driving gravity center migration

Since the CEGC migration of RRB showed obvious reverse migration characteristics after 2013, this study analyzed the causes of gravity center migration during three time periods: 2005–2010; 2010–2013; and 2013–2018. In order to further judge the comprehensive contribution of each region to the CEGC, this paper unifies the migration direction and amount of gravity center into the same coordinate (Fig. 6) to make comparison from the geographical location and migration direction of each region, the

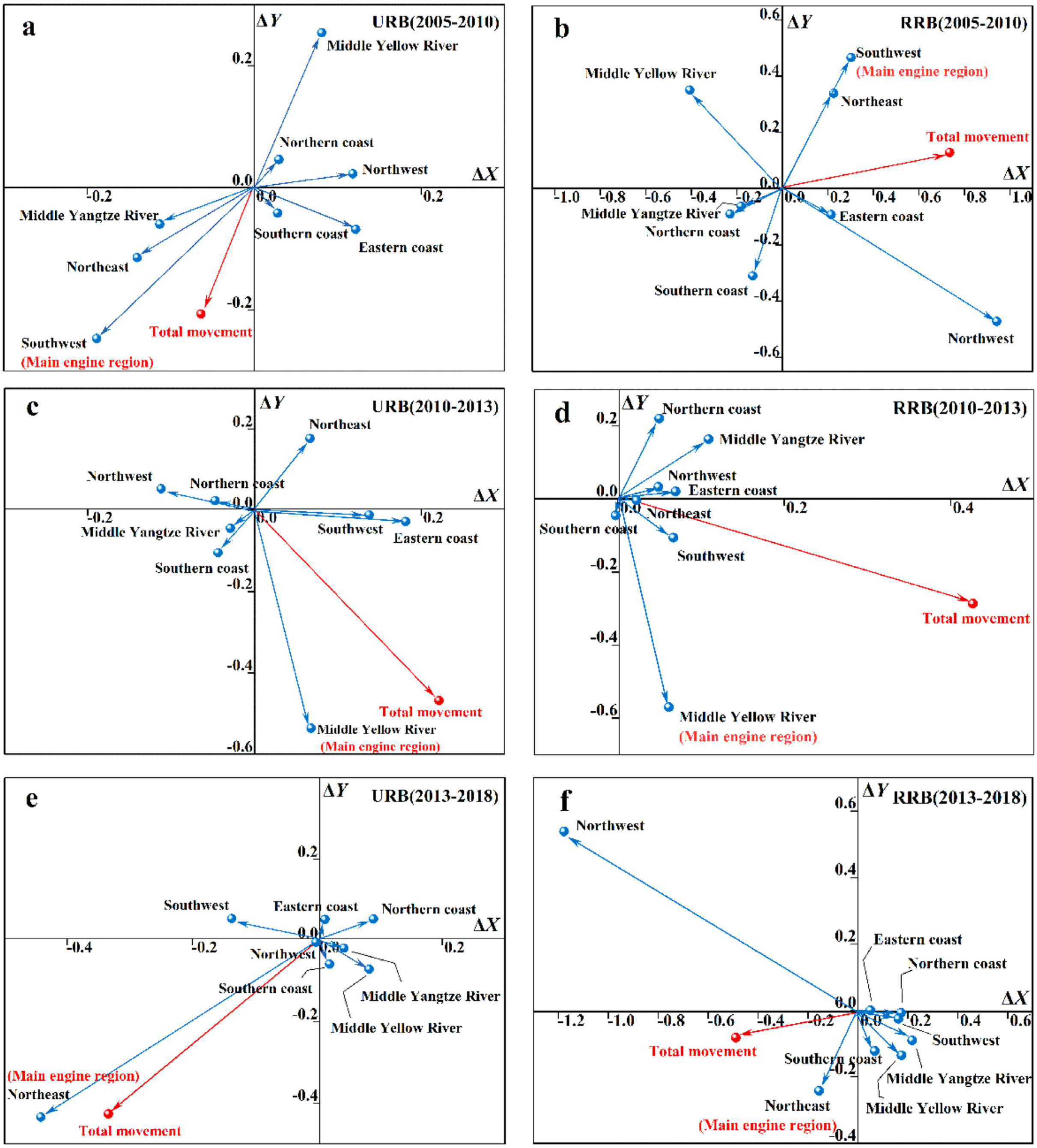

Fig. 6. Regional contribution of CEGC migration of URB and RRB in different periods.

region which makes a positive contribution was defined as the "engine region" (Song and Zhang, 2019). Then Fig. 7 shows the results of ST-LMDI decomposition and explains the contribution of every driving factor to the change of carbon emissions in each region.

First stage (2005–2010): During this stage, the southwest acted as the main engine region for the migration of the CEGC of URB (Fig. 6a). This was due to the fact that the southwest showed the largest increase in carbon emissions during this period, with a growth rate of 44%. Except for *EE*, all other factors promoted the growth of URB-related emission in the southwest region, where *EI*, *PY* and *P* were the main contributing factors (Fig. 7a). Furthermore, except for the northeast and northwest regions, the force direction of other regions on the emission gravity center of URB was consistent with the relative direction of geographical locations during this stage, indicating that during the 11th Five-Year Plan period, the urbanization levels of most regions in China were in a stage of rapid development, and that the overall URB-related carbon emissions were growing rapidly.

During this stage, the CEGC of RRB migrated to the northeast, the southwest and northwest being the main engine regions for latitude and longitude-related movements, respectively (Fig. 6b). This is because RRB-related carbon emissions in the southwest and northwest regions decreased by 11.69% and 13.20%, respectively, while those of the remaining regions displayed an increasing trend. *EE* and *EI* were the main factors causing a reduction in RRB-related carbon emissions in the northwest during this stage, with *P* and *EE* being the main driving factors for same in the southwest (Fig. 7b). Compared with that in other regions, the

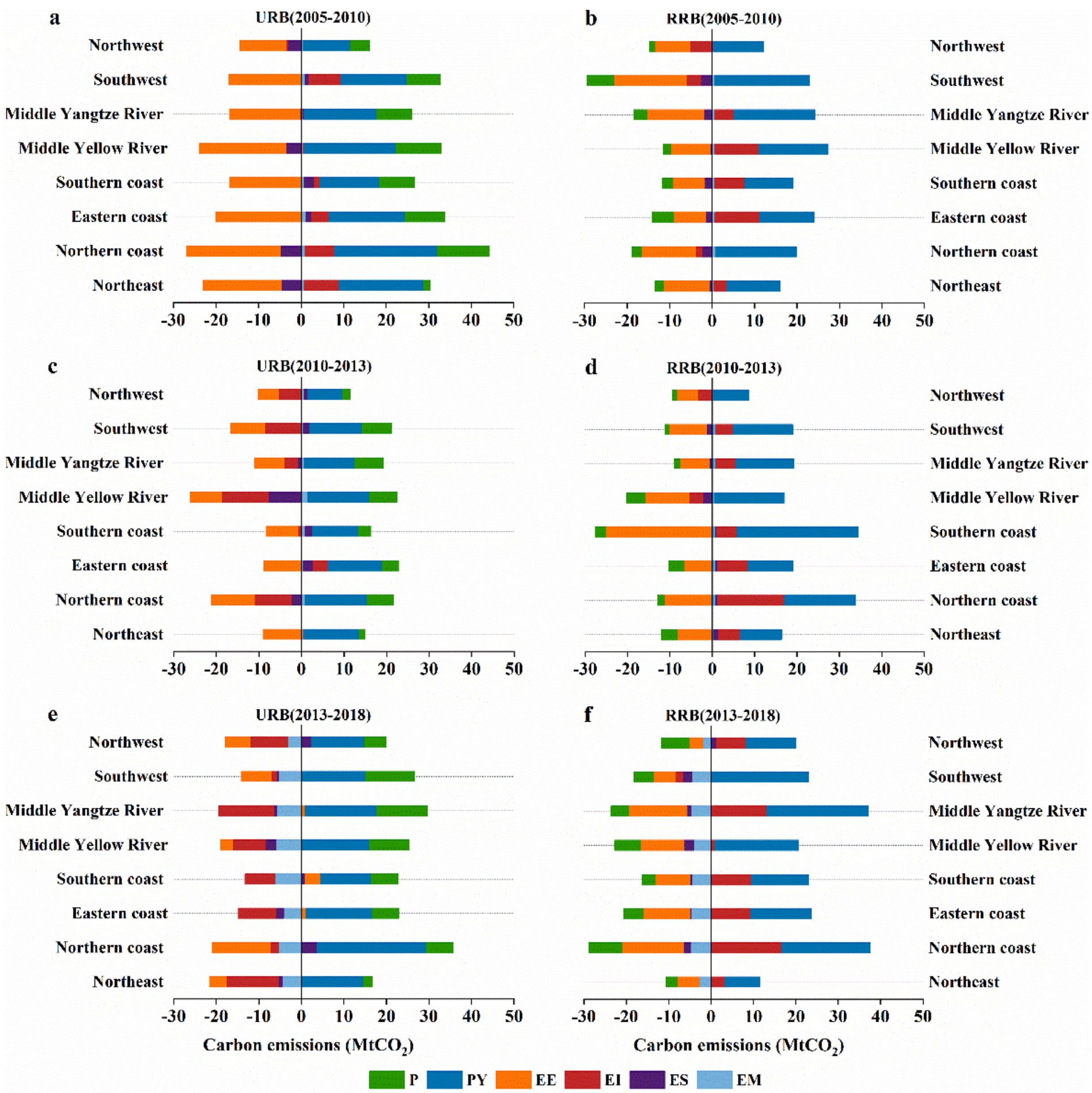

Fig. 7. Decomposition results of carbon emission change drivers of URB and RRB in different regions.

above-mentioned two factors exerted the strongest negative effect on RRB-related carbon emissions in the southwest, implying that the rural population and floor space of residential buildings in the southwest decreased the most during this stage, which may account for increased population attraction for the southwestern urban areas.

Second stage (2010–2013): During this stage, the main engine region driving the migration of CEGCs of both URB and RRB was middle Yellow River (Fig. 6c, d). This was due to a significant decline in residential building-related carbon emissions. Compared with those in 2010, the URB-related carbon emissions in this region decreased by 365.13 Mt CO_2 in 2013, this being the only region where URB-related carbon emissions decreased during this stage. The decline in *EI* and optimization of *ES* were the main factors driving the reduction in URB-related emissions in this region (Fig. 7c), which is likely attributed to the effectiveness of the issue in prompting the retrofitting of the existing residential buildings in China's northern heating region during the 11th Five Year Plan.

RRB-related carbon emissions of the middle Yellow River decreased by 325.91 Mt CO_2 during this stage, with this region being the one showing the largest reduction; a loss in rural population and a slowdown of *EE* were the main factors that were suggested as being responsible for the negative emissions. Meanwhile, *EI* and *ES* also inhibited the increase in RRB-related emissions to a certain extent (Fig. 7d). Furthermore, with respect to the eastward migration of the gravity center during this stage, the changes in RRB-related emissions in the other seven regions, except for the weak reaction force in the southern coast region, promoted eastward movement of the gravity center, indicating that after entering the 12th Five Year Plan development period, the speed of rural development in the eastern region was significantly higher than that in the western region.

Third stage (2013–2018): During this stage, the northeast acted as the main engine region driving the migration of the CEGC of the URB towards the southwest (Fig. 6e). This was because the northeast had become the only region where URB-related emissions decreased by 8%, the reduction in *EI* being the main factor causing the decline in URB-related emissions in the northeast during this period (Fig. 7e). In addition, due to a slowdown in the average annual growth rate of URB-related emissions in each region during this period, the effect of the remaining seven regions on the center of gravity was weakened compared with those in the first two stages, indicating that the growth trend shown by URB-related carbon emissions had slowed down during this period.

During this period, the CEGC of the RRB moved towards the southwest. The northeast and northwest regions acted as the main engine regions causing a latitude- and longitude-based change in the gravity center, respectively (Fig. 6f). This change was attributed to the fact that the northwest region showed the largest growth rate in URB-related emissions, compared with those of other regions, which reached 51.40%, as well as that of the URB of the northeast region, which only increased by 84.91 Mt CO_2., with the weakest growth rate being 4%. *EI* and *PY* were the main factors promoting the growth of RRB-related emission in the northwest region, and compared with that in other regions, *EE* exerted the weakest inhibition effect on RRB-related carbon emission in the northwest region (Fig. 7f), which indicated that the level of rural development in the northwest had begun to accelerate. By contrast, rural economic development in the northeast region was relatively slow. Compared with that in other stages, the average annual growth rate of *PY* in the northeast region was reduced to 5%, while the average growth rate of *PY* in China during this period was 10.07%. Therefore, the weakening of *PY* effect likely played an important role in slowing down RRB-related emission growth in the northeast region.

4. Discussion

4.1. What causes the difference in the migration of CEGC between URB and RRB?

To further explore the mechanism underlying the difference in CEGC migration between URB and RRB, we determined the dominant reason by calculating the sum of the absolute contribution rates for all periods of each region and driving factor respectively (Fig. 8). The absolute contribution rates of regions ($|SR_X + SR_Y|$) indicated that each region makes a relatively uniform contribution to the movement of the CEGC of URB, with the northeast region being the one that contributes the greatest force (Fig. 8a). By contrast, the contribution of each region to CEGC track movement of the RRB exhibited a sharp difference (Fig. 8b), with the northwest playing a leading role, which indicated that the change of carbon emissions in RRB has a more distinctive function of strong spatial heterogeneity as well as spatial distribution compared with URB.

According to the absolute contribution rate of factors ($|CR|$), *PY* and *EE* are the factors that play an important role in causing a change in the CEGC of URB and RRB in three periods, indicating that the floor space and economic level show the highest level of correlation with the movement of the CEGC. Specifically, the population effect in the northeast, the main engine region that drives the CEGC of URB southward, was obviously weaker than that in other regions (Fig. 8a). According to statistics, the population in the northeast decreased by 1.2% compared with that in 2010, implying that weakening population attractiveness is occurring in the northeast (Jin et al., 2022), which might play a major role in the reduction in URB. By contrast, the effect of *EI* on RRB-related emission in the northwest changed from inhibition to promotion and the absolute contribution rate was highest among all regions (Fig. 8b). Thus, the shapely effect transformation of *EI* appears to be the critical reason behind the large emission change in RRB in the northwest.

4.2. What is the migration trend of the two gravity center tracks in the future?

The Tapio decoupling model applied in this study aimed to determine the future movement trends of the CEGC (issue 4 stated in the introduction). The income of residents is the primary factor affecting the change in residential building carbon emissions in each region. The decoupling model can accurately judge whether there is a coupling relationship between economic growth and carbon emissions and the strength of the coupling state, which is helpful for evaluating the future development trend of carbon emissions in various regions (Wenbo and Yan, 2018). Therefore, this study adopted a more flexible and stable Tapio decoupling model (Chen et al., 2018) to calculate decoupling elasticity between carbon emissions of two types of residential buildings and the per capita income of residents in each region. The calculation model is as follows:

$$\varphi = \frac{\Delta C/C_0}{\Delta PY/PY_0} = \frac{(C_T - C_0)/C_0}{(PY_T - PY_0)/PY_0} \tag{17}$$

where φ indicates the elasticity coefficient, C_0, C_T represent the carbon emissions in the base and final periods, respectively, and PY_0, PY_T represent the per capita income of residents in the corresponding period, and the final results are shown in Fig. 9.

According to the value of φ, the decoupling state can be divided into three categories: decoupling, negative coupling, and coupling. Each category contains different substates (Fig. 9a). Among these, strong decoupling represents the most ideal state, indicating that income growth of residents will no longer be at the cost of increasing carbon emissions, and strong negative decoupling represents the worst result (Wenbo and Yan, 2018).

The decoupling status of the URB and RRB in various regions during different periods is shown in Fig. 9b. Evidently, most regions were in a weak decoupling state from 2005 to 2010, with only a few rural areas, such as the northwest and southwest regions, showing strong decoupling levels, which gradually changed to weak decoupling or expansive coupling with regional development. During the period from 2010 to 2013, the difference in the decoupling levels among regions became larger, and the number of regions showing expansive coupling and strong decoupling levels increased. Finally, the decoupling states of most regions reached weak decoupling levels after 2013. The overall results indicated that the association between carbon emissions from residential buildings and the income of residents in China has not reached the ideal decoupling state, which is consistent with the conclusions of existing research studies at the provincial level (Huo et al., 2019; Liang et al., 2019).

With respect to URB, all regions, except the northeast, had reached a weak decoupling state following fluctuations with a small gap, implying that, as the income of residents reaches higher levels in the future, the increase in the range of URB in most regions would drop, and that both the speed and direction of movement will not change significantly. The association between carbon emissions and *PY* has reached a strong decoupling state under the dilemma of recession and imbalance that many cities in the northeast are facing, and the emission growth trend of URB in this region will probably continue to decline. Therefore, as the income levels of urban residents improve, the CEGC of URB will likely continue to move slowly towards the southwest under the promotion of the northeast and the relatively balanced forces from other regions.

With respect to RRB, the decoupling status in the more developed rural areas, such as the southeast coast and the middle Yangtze River, was basically consistent with that of URB, while that in rural areas with large rural populations or large proportions, such as the northern coast, the middle Yellow River,

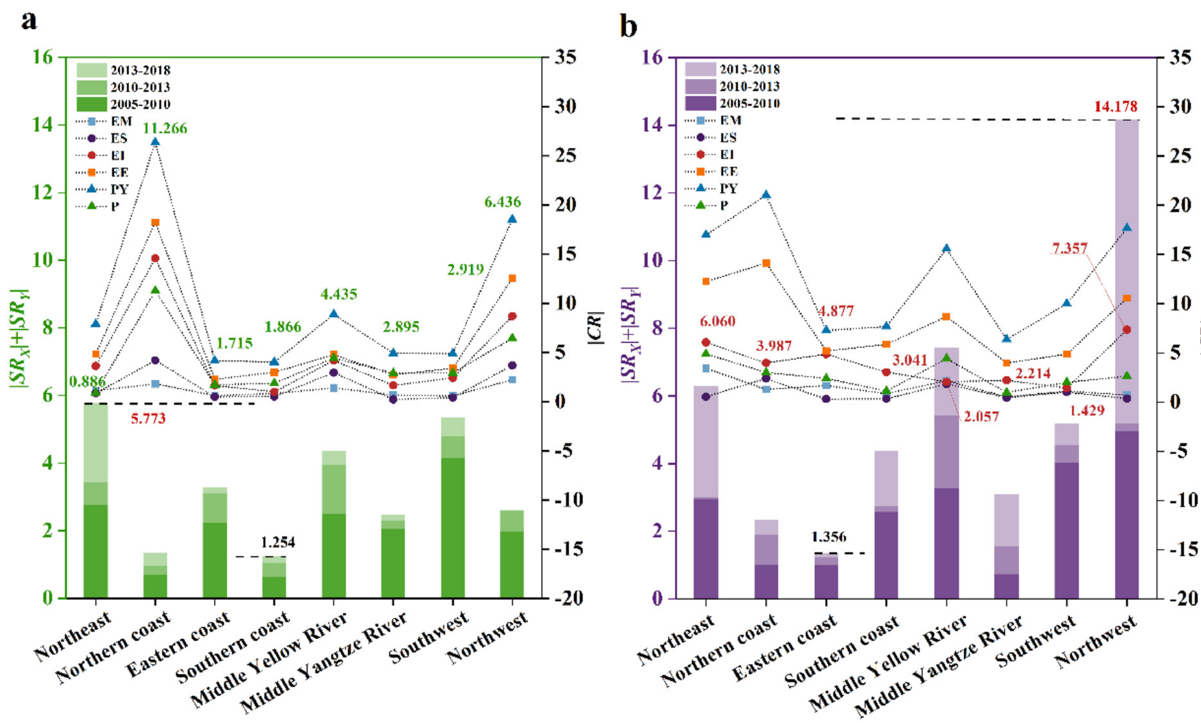

Fig. 8. Absolute contribution rate of regions and driving factors for CEGC movement of URB (a) and RRB (b).

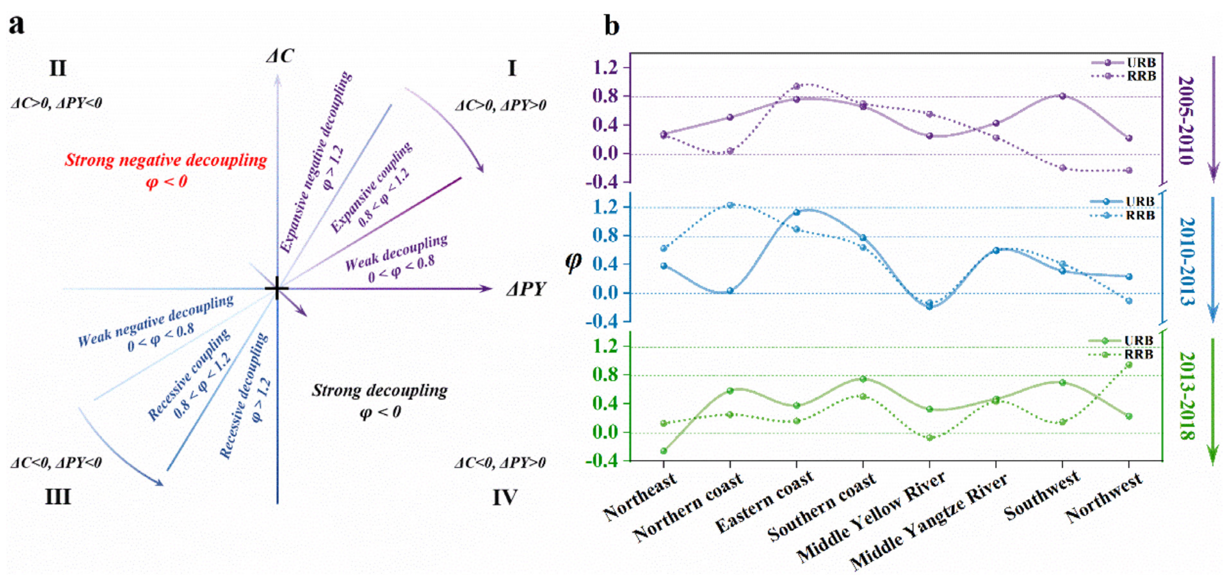

Fig. 9. Decoupling states (a) and results (b) of carbon emissions and *PY*.

and the northwest, was obviously out of sync with the URB. Specifically, due to the low level of urbanization in northwestern China, the state of decoupling between carbon emissions and RRB has lagged behind. Since the implementation of China's Western Development Policy in 2000, the economy of the western area has undergone steady and rapid development. After 2012, the average annual growth rate of gross domestic product in the western area reached 8.9%, a value higher than that of the national average growth rate, the above situation has driven the development of rural areas in the northwestern region. Thus, the decoupling state of RRB-related emissions in the northwest changes from a strong decoupling state to an expansive coupling state, while that of other regions remains as a weak decoupling or strong decoupling state. Therefore, in the next period, the CEGC of the RRB will mainly be driven by the northwest and maintain its trend of moving westward, with an even larger probability of moving to the northwest.

5. Conclusions and future research directions

5.1. Main conclusions

This study explored the spatial evolution law governing different types of residential buildings using the gravity center model and quantified the factors driving the migration of gravity centers, in combination with the two kinds of decomposition models. Furthermore, we analyzed the decoupling state of carbon emissions and *PY* and forecasted future development trends. The main resolutions to the four issues raised by this study are as follows: (1) The CEGC track of residential buildings shows a southward trend. The overall CEGC of the URB moves to the southwest, while the emission gravity center of the RRB moves first to the southeast and then to the southwest, with an average moving speed that is higher than that of the URB. (2) Differences were evident between the main engine regions affecting the movement of the carbon emission gravity center of the URB and RRB in each stage. The southwest, middle Yellow River, and northeast became the main engine regions driving CEGC movement of URB at each stage; the southwest and northwest, the middle Yellow River, northeast, and northwest were the regions, or combinations of regions, that exerted a great effect on the CEGC shift in RRB at each stage, while the northeast and northwest regions acted as the largest driving factors in the CEGC movement of the URB and RRB, respectively. (3) *PY*, *EI*, and *EE* are the main drivers of the CEGC movement in residential buildings. These three factors played an important role in changing residential area-related carbon emissions. *PY* exerted a positive effect on the growth of carbon emissions, while *EE* exerted a negative effect. *EI* inhibited the growth of URB-related carbon emission but promoted that of RRB-related emissions. (4) Under the influence of *PY*, the CEGC of both URB and RRB showed the trend of moving westward. As *PY* increases, the emission gravity center of the URB continues to move to the southwest, while that of the RRB moves to the northwest.

Expectedly, the conclusions of this study may not only help better understand the differences between the spatial distribution of carbon emissions of different types of residential buildings but may also reflect the current situation of urban and rural regional development in China. The main policy impacts are as follows: (1) Attention should be paid to building energy conservation in rural areas. Compared with that of URB, the *EI* of RRB did not show an obvious inflection point, and its coupling level with *PY* was relatively high. With the westward movement of the CEGC of RRB, carbon emissions will have a greater impact on the environment of the western region. Therefore, the government should formulate policies for energy-saving construction and transformation that are able to adapt to the complex energy consumption patterns in rural areas, and thereby help reduce emission peak values of RRB, balance economic growth and enhance ecological sustainability in rural areas. (2) In the process of promoting the decoupling of carbon emissions and *PY*, the government should adjust policy priorities according to the development status of different regions. The southern provinces with demographic and economic attractiveness can continue to implement higher energy-saving standards. Northeast provinces need reasonable talent incentive policies to stimulate economic vitality and ensure reasonable mitigation of carbon emissions under the premise of steady economic growth.

5.2. Future research directions

Several limitations that beset this study may need to be addressed by future research studies attempting to obtain a comprehensive understanding of the spatial–temporal evolution law governing carbon emissions in buildings. Firstly, building type analysis needs to be extended. Although this study explored the spatial–temporal evolution law governing the residential building sector in China, the specific spatial–temporal characteristics of the public building sector in China, which is associated with even higher emission levels, is also worthy of evaluation via the methods applied in this study. Secondly, the dimensions of influencing factors need to be extended. Because this study explored the spatial–temporal evolution law governing the residential building sector in China, which is more closely related to resident live, thus some social factors are also worthy of evaluation via the methods applied in this study. Finally, the divisive criteria of regions that contribute to the spatial–temporal evolution of emission may be changed according to specific policy purposes. In addition to the economic zones assessed in this study, the zone related to the climate (e.g., building climate zones) should also be taken into consideration; furthermore, the contributions of different counties to the spatial–temporal evolution of carbon emissions should also be taken into consideration when conducting analyses at the global level.

CRediT authorship contribution statement

Jiebing Wang: Methodology, Formal analysis, Data curation, Visualization. **Kairui You:** Conceptualization, Supervision, Formal analysis, Methodology. **Lingling Qi:** Data curation, Visualization, Writing – review & editing. **Hong Ren:** Writing – review & editing, Supervision.

Declaration of competing interest

The authors declare that they have no known competing financial interests or personal relationships that could have appeared to influence the work reported in this paper.

Acknowledgments

The authors would like to acknowledge financial support provided by Chongqing Graduate Research innovation Project (CYS21035).

References

Ang, B.W., Su, B., Wang, H., 2016. A spatial–Temporal decomposition approach to performance assessment in energy and emissions. Energy Econ. 60, 112–121. http://dx.doi.org/10.1016/j.eneco.2016.08.024.

Balsa-Barreiro, J., Li, Y., Morales, A., Pentland, A.S., 2019. Globalization and the shifting centers of gravity of world's human dynamics: Implications for sustainability. J. Clean. Prod. 239, 117923. http://dx.doi.org/10.1016/j.jclepro.2019.117923.

CABEE, 2020. China Building Energy Consumption. Report (2020), China Association of Building Energy Efficiency, Beijing, Available at: https://24959527.s21i.faiusr.com/61/ABUIABA9GAAguJHP-wUozLXhgwM.pdf.

Chen, H., Chen, W., 2019. Carbon mitigation of China's building sector on city-level: Pathway and policy implications by a low-carbon province case study. J. Clean. Prod. 224, 207–217. http://dx.doi.org/10.1016/j.jclepro.2018.12.022.

Chen, J., Wang, P., Cui, L., Huang, S., Song, M., 2018. Decomposition and decoupling analysis of CO2 emissions in OECD. Appl. Energy 231, 937–950. http://dx.doi.org/10.1016/j.apenergy.2018.09.179.

Cong, X., Zhao, M., Li, L., 2015. Analysis of carbon dioxide emissions of buildings in different regions of China based on STIRPAT model. Proc. Eng. 121, 645–652. http://dx.doi.org/10.1016/j.proeng.2015.08.1057.

Delmastro, C., Lavagno, E., Mutani, G., 2015. Chinese residential energy demand: Scenarios to 2030 and policies implication. Energy Build. 89, 49–60. http://dx.doi.org/10.1016/j.enbuild.2014.12.004.

Fan, W., Li, L., Wang, F., Li, D., 2020. Driving factors of CO2 emission inequality in China: The role of government expenditure. China Econ. Rev. 64, http://dx.doi.org/10.1016/j.chieco.2020.101545.

Fu, J., Gao, Z., Huang, L., Zhang, L., 2011. The movement route of consumption gravity center of Xinjiang from 1965 to 2009 based on GIS. Earth Planet. Sci. 2, 321–326. http://dx.doi.org/10.1016/j.proeps.2011.09.050.

Grether, J.M., Mathys, N.A., 2010. Is the world's economic centre of gravity already in Asia? Gen. Introd. Geogr. 42, 47–50. http://dx.doi.org/10.1111/j.1475-4762.2009.00895.x.

Halleck Vega, S., van Leeuwen, E., van Twillert, N., 2022. Uptake of residential energy efficiency measures and renewable energy: Do spatial factors matter? Energy Policy 160, 112659. http://dx.doi.org/10.1016/j.enpol.2021.112659.

Han, L., Xu, X., Han, L., 2015. Applying quantile regression and Shapley decomposition to analyzing the determinants of household embedded carbon emissions: Evidence from urban China. J. Clean. Prod. 103, 219–230. http://dx.doi.org/10.1016/j.jclepro.2014.08.078.

Harris, I., Naim, M., Palmer, A., Potter, A., Mumford, C., 2011. Assessing the impact of cost optimization based on infrastructure modelling on CO2 emissions. Int. J. Prod. Econ. 131, 313–321. http://dx.doi.org/10.1016/j.ijpe.2010.03.005.
Huo, T., Cai, W., Ren, H., Feng, W., Zhu, M., Lang, N., Gao, J., 2019. China's building stock estimation and energy intensity analysis. J. Clean. Prod. 207, 801–813. http://dx.doi.org/10.1016/j.jclepro.2018.10.060.
Huo, T., Cao, R., Du, H., Zhang, J., Cai, W., Liu, B., 2021a. Nonlinear influence of urbanization on China's urban residential building carbon emissions: New evidence from panel threshold model. Sci. Total Environ 772, 145058. http://dx.doi.org/10.1016/j.scitotenv.2021.145058.
Huo, T., Li, X., Cai, W., Zuo, J., Jia, F., Wei, H., 2020. Exploring the impact of urbanization on urban building carbon emissions in China: Evidence from a provincial panel data model. Sustain. Cities Soc. 56, 102068. http://dx.doi.org/10.1016/j.scs.2020.102068.
Huo, T., Ma, Y., Yu, T., Cai, W., Liu, B., Ren, H., 2021b. Decoupling and decomposition analysis of residential building carbon emissions from residential income: Evidence from the provincial level in China. Environ. Impact Assess. Rev. 86, 106487. http://dx.doi.org/10.1016/j.eiar.2020.106487.
Huo, T., Ren, H., Zhang, X., Cai, W., Feng, W., Zhou, N., Wang, X., 2018. China's energy consumption in the building sector: A statistical yearbook-energy balance sheet based splitting method. J. Clean. Prod. 185, 665–679. http://dx.doi.org/10.1016/j.jclepro.2018.02.283.
Jiang, S., Zhu, Y., He, G., Wang, Q., Lu, Y., 2020. Factors influencing China's non-residential power consumption: Estimation using the Kaya–LMDI methods. Energy 201, 117719. http://dx.doi.org/10.1016/j.energy.2020.117719.
Jin, C., Li, B., Jansen, S.J.T., Boumeester, H.J.F.M., Boelhouwer, P.J., 2022. What attracts young talents? Understanding the migration intention of university students to first-tier cities in China. Cities 128, 103802. http://dx.doi.org/10.1016/j.cities.2022.103802.
Kaya, Y., 1989. Impact of carbon dioxide emission control on GNP growth: interpretation of proposed scenarios. Intergovernmental Panel on Climate Change/Response Strategies Working Group, May. Available at: https://archive.ipcc.ch/publications_and_data/publications_ipcc_first_assessment_1990_wg3.shtml.
Li, Z., Luan, W., Zhang, Z., Su, M., 2020b. Relationship between urban construction land expansion and population/economic growth in Liaoning Province, China. Land Use Policy. 99, 105022. http://dx.doi.org/10.1016/j.landusepol.2020.105022.
Li, K., Ma, M., Xiang, X., Feng, W., Ma, Z., Cai, W., Ma, X., 2022. Carbon reduction in commercial building operations: A provincial retrospection in China. Appl. Energy 306, 118098. http://dx.doi.org/10.1016/j.apenergy.2021.118098.
Li, H., Qiu, P., Wu, T., 2021a. The regional disparity of per-capita CO2 emissions in China's building sector: An analysis of macroeconomic drivers and policy implications. Energy Build. 244, 111011. http://dx.doi.org/10.1016/j.enbuild.2021.111011.
Li, X., Wang, J., Zhang, M., Ouyang, J., Shi, W., 2020a. Regional differences in carbon emission of China's industries and its decomposition effects. J. Clean. Prod. 270, 122528. http://dx.doi.org/10.1016/j.jclepro.2020.122528.
Li, Z., Zhao, T., Wang, J., Cui, X., 2021b. Two-step allocation of CO2 emission quotas in China based on multi-principles: Going regional to provincial. J. Clean. Prod. 305, 127173. http://dx.doi.org/10.1016/j.jclepro.2021.127173.
Liang, Y., Cai, W., Ma, M., 2019. Carbon dioxide intensity and income level in the Chinese megacities' residential building sector: Decomposition and decoupling analyses. Sci. Total Environ. 677, 315–327. http://dx.doi.org/10.1016/j.scitotenv.2019.04.289.
Liang, L., Chen, M., Luo, X., Xian, Y., 2021. Changes pattern in the population and economic gravity centers since the reform and opening up in China: The widening gaps between the South and North. J. Clean. Prod. 310, 127379. http://dx.doi.org/10.1016/j.jclepro.2021.127379.
Liu, J., Wang, M., 2019. Study on calculation and regional difference of carbon emission of urban civil buildings in China. In: 3rd International Workshop on Advances in Energy Science and Environment Engineering. AESEE, Suzhou, PEOPLES R CHINA, http://dx.doi.org/10.1063/1.5109350.
Ma, L., Long, H., Chen, K., Tu, S., Zhang, Y., Liao, L., 2019. Green growth efficiency of Chinese cities and its spatio-temporal pattern. Resour. Conserv. Recycl. 146, 441–451. http://dx.doi.org/10.1016/j.resconrec.2019.03.049.
Ma, M., Ma, X., Cai, W., Cai, W., 2020. Low carbon roadmap of residential building sector in China: Historical mitigation and prospective peak. Appl. Energy 273, 115247. http://dx.doi.org/10.1016/j.apenergy.2020.115247.
McNeil, M.A., Feng, W., Can, S.de.la.Rue.du., Khanna, N.Z., Ke, J., Zhou, N., 2016. Energy efficiency outlook in China's urban buildings sector through 2030. Energy Policy 97, 532–539. http://dx.doi.org/10.1016/j.enpol.2016.07.033.
Meng, G., Guo, Z., Li, J., 2021. The dynamic linkage among urbanisation, industrialisation and carbon emissions in China: Insights from spatiotemporal effect. Sci. Total Environ. 760, 144042. http://dx.doi.org/10.1016/j.scitotenv.2020.144042.
NBS, 2019. China Statistical Yearbook (2001-2018). National Bureau of Statist, Available at: http://www.stats.gov.cn/tjsj/ndsj/.
Schäuble, D., Marian, A., Cremonese, L., 2020. Conditions for a cost-effective application of smart thermostat systems in residential buildings. Appl. Energy 262, 114526. http://dx.doi.org/10.1016/j.apenergy.2020.114526.
Shapley, L., 1953. In: Kuhn, H.W., Tucker, A.W. (Eds.), A Value for N-Person Games. Princeton University Press, Princeton.
Shi, Q., Gao, J., Wang, X., Ren, H., Cai, W., Wei, H., 2020. Temporal and spatial variability of carbon emission intensity of urban residential buildings: Testing the effect of economics and geographic location in China. Sustainability 12 (7), 2695. http://dx.doi.org/10.3390/su12072695.
Shi, Y., Han, B., Han, L., Wei, Z., 2019. Uncovering the national and regional household carbon emissions in China using temporal and spatial decomposition analysis models. J. Clean. Prod. 232, 966–979. http://dx.doi.org/10.1016/j.jclepro.2019.05.302.
Shorrocks, A.F., 1999. Decomposition Procedures for Distributional Analysis: A Unified Framework Based on the Shapley Value. University of Essex, Mimeo.
Song, Y., Zhang, M., 2019. Research on the gravity movement and mitigation potential of Asia's carbon dioxide emissions. Energy 170, 31–39. http://dx.doi.org/10.1016/j.energy.2018.12.110.
Sun, X., Li, Z., Cheng, X., Guan, C., Han, M., Zhang, B., 2022. Global anthropogenic CH4 emissions from 1970 to 2018: Gravity movement and decoupling evolution. Resour. Conserv. Recycl. 182, 106335. http://dx.doi.org/10.1016/j.resconrec.2022.106335.
Tan, X., Lai, H., Gu, B., Zeng, Y., Li, H., 2018. Carbon emission and abatement potential outlook in China's building sector through 2050. Energy Policy 118, 429–439. http://dx.doi.org/10.1016/j.enpol.2018.03.072.
THUBERC, 2020. Annual Development Research Report on Building Energy Efficiency in China (2020). China Architecture & Building Press, Beijing.
Wang, C., Guo, Y., Shao, S., Fan, M., Chen, S., 2020a. Regional carbon imbalance within China: An application of the kaya-zenga index. J. Environ. Manage 262, 110378.
Wang, R., Wang, Q., Yao, S., 2021. Evaluation and difference analysis of regional energy efficiency in China under the carbon neutrality targets: Insights from DEA and theil models. J. Environ. Manage 293, 112958. http://dx.doi.org/10.1016/j.jenvman.2021.112958.
Wang, K., Zhao, X., Peng, B., Zeng, Y., 2020b. Spatio-temporal pattern and driving factors of municipal solid waste generation in China: New evidence from exploratory spatial data analysis and dynamic spatial models. J. Environ. Manage 262, 110378. http://dx.doi.org/10.1016/j.jenvman.2020.110378.
Wen, Q., Chen, Y., Hong, J., Chen, Y., Ni, D., Shen, Q., 2020. Spillover effect of technological innovation on CO2 emissions in China's construction industry. Build. Environ. 171, 106653. http://dx.doi.org/10.1016/j.buildenv.2020.106653.
Wenbo, G., Yan, C., 2018. Assessing the efficiency of China's environmental regulation on carbon emissions based on Tapio decoupling models and GMM models. Energy Rep. 4, 713–723. http://dx.doi.org/10.1016/j.egyr.2018.10.007.
Wu, Y., Shi, X., Hu, C., 2021b. Per capita CO2 emissions divergence influenced by bilateral trade with china under the belt and road initiative. Sustain. Prod. Consum. 27, 1589–1601. http://dx.doi.org/10.1016/j.spc.2021.04.005.
Wu, R., Wang, J., Wang, S., Feng, K., 2021a. The drivers of declining CO2 emissions trends in developed nations using an extended STIRPAT model: A historical and prospective analysis. Renew. Sustain. Energy Rev. 149, 111328. http://dx.doi.org/10.1016/j.rser.2021.111328.
Yan, J., Yang, Y., Campana, P.E., He, J., 2019. City-level analysis of subsidy-free solar photovoltaic electricity price, profits and grid parity in China. Nat Energy. 4 (8), 709–717. http://dx.doi.org/10.1038/s41560-019-0441-z.
You, K., Yu, Y., Li, Y., Cai, W., Shi, Q., 2021. Spatiotemporal decomposition analysis of carbon emissions on Chinese residential central heating. E Energy Build. 253, 111485. http://dx.doi.org/10.1016/j.enbuild.2021.111485.
Yu, S., Wei, Y.-M., Wang, K., 2014. Provincial allocation of carbon emission reduction targets in China: An approach based on improved fuzzy cluster and Shapley value decomposition. Energy Policy 66, 630–644. http://dx.doi.org/10.1016/j.enpol.2013.11.025.
Zhang, X., Geng, Y., Tong, Y.W., Kua, H.W., Tian, X., Wu, R., Zhao, X., Chiu, A.S.F., 2021. Spatial characteristics and its driving factors of low-carbon energy technology innovation in China: A gravity movement and exploratory spatial data analysis. J. Clean. Prod. 295, 126481. http://dx.doi.org/10.1016/j.jclepro.2021.126481.
Zhang, X., Wang, F., 2017. Life-cycle carbon emission assessment and permit allocation methods: A multi-region case study of China's construction sector. Ecol. Indic. 72, 910–920. http://dx.doi.org/10.1016/j.ecolind.2016.09.023.
Zhang, Y.-J., Wang, A.-D., Da, Y.-B., 2014. Regional allocation of carbon emission quotas in China: Evidence from the Shapley value method. Energy Policy 74, 454–464. http://dx.doi.org/10.1016/j.enpol.2014.08.006.
Zhang, Y., Zhang, J., Yang, Z., Li, J., 2012. Analysis of the distribution and evolution of energy supply and demand centers of gravity in China. Energy Policy 49, 695–706. http://dx.doi.org/10.1016/j.enpol.2012.07.012.
Zhou, N., Khanna, N., Feng, W., Ke, J., Levine, M., 2018. Scenarios of energy efficiency and CO2 emissions reduction potential in the buildings sector in China to year 2050. Nat. Energy 3, 978–984. http://dx.doi.org/10.1038/s41560-018-0253-6.